

Article

Production of Bio-Oil from De-Oiled Karanja (*Pongamia pinnata* L.) Seed Press Cake via Pyrolysis: Kinetics and Evaluation of Anthill as the Catalyst

Jan Nisar ^{1,*}, Salman Waris ¹, Afzal Shah ^{2,*}, Farooq Anwar ³, Ghulam Ali ¹, Ali Ahmad ¹ and Faisal Muhammad ¹

- ¹ National Centre of Excellence in Physical Chemistry, University of Peshawar, Peshawar 25120, Pakistan; salmanwaris5544@gmail.com (S.W.); ghulamali@uop.edu.pk (G.A.); aliahmaddawar485@gmail.com (A.A.); faisalmuhammad77318@gmail.com (F.M.)
- ² Department of Chemistry, Quaid-i-Azam University, Islamabad 45320, Pakistan
- ³ Institute of Chemistry, University of Sargodha, Sargodha 40100, Pakistan; fqanwar@yahoo.com
- * Correspondence: pashkalawati@gmail.com or jan_nisar@uop.edu.pk (J.N.); afzalshah@qau.edu.pk or afzals_qau@yahoo.com (A.S.)

Abstract: In this study, bio-oil was produced from the pyrolysis of de-oiled karanja seed press cake in the presence of abandoned anthill as the catalyst. The anthill was characterised by SEM, EDX, XRF, XRD and surface area and pore size analysis. The pyrolysis experiments were carried out in an indigenously made furnace in a nitrogen atmosphere from 310 to 400 °C. The pyrolysis oil was collected at an optimised temperature and analysed through gas chromatography–mass spectrometry (GC-MS). The compounds identified via GC-MS of non-catalytic bio-oil were in the range of C₅ to C₁₉, and compounds identified from catalytic bio-oil were in the range of C₂–C₆₃. Furthermore, thermogravimetric analysis of the karanja seed press cake without and with anthill was carried out in a nitrogen atmosphere with temperature programme rates of 3, 12, 20 and 30 °C·min⁻¹. Kinetic parameters were determined by applying the Kissinger equation. The activation energy (E_a) values for hemicelluloses, cellulose and lignin were obtained as 99.7 ± 0.4, 182.9 ± 0.5 and 199.5 ± 0.7 kJ·mol⁻¹ without catalyst; and with catalyst, the E_a were lowered to 74.8 ± 0.2, 83.1 ± 0.4 and 108.0 ± 0.5 kJ·mol⁻¹, respectively. From the results, it was concluded that the catalyst played a key role in lowering the activation energy for the pyrolysis reaction and enhanced the quality of the bio-oil obtained as well.

Keywords: *Pongamia pinnata* L.; press cake; anthill; pyrolysis; kinetics; activation energy; thermo-gravimetric analysis



Citation: Nisar, J.; Waris, S.; Shah, A.; Anwar, F.; Ali, G.; Ahmad, A.; Muhammad, F. Production of Bio-Oil from De-Oiled Karanja (*Pongamia pinnata* L.) Seed Press Cake via Pyrolysis: Kinetics and Evaluation of Anthill as the Catalyst. *Sustain. Chem.* **2022**, *3*, 345–357. <https://doi.org/10.3390/suschem3030022>

Academic Editor: James A. Sullivan

Received: 15 May 2022

Accepted: 25 July 2022

Published: 27 July 2022

Publisher's Note: MDPI stays neutral with regard to jurisdictional claims in published maps and institutional affiliations.



Copyright: © 2022 by the authors. Licensee MDPI, Basel, Switzerland. This article is an open access article distributed under the terms and conditions of the Creative Commons Attribution (CC BY) license (<https://creativecommons.org/licenses/by/4.0/>).

1. Introduction

Energy plays a major role in the economy of a nation, and energy assets have direct impacts on the stability and prosperity of a nation. The energy assets include nuclear fossil fuels and renewable resources [1]. Presently, almost 13% of the world's energy demand is fulfilled by nuclear energy, and more than 400 nuclear power stations are active worldwide [2]. As a result of energy production from nuclear power plants, radioactive waste is produced, which is dangerous for plants, animals and the whole ecosystem [3].

Moreover, fossil fuels are primary sources of energy, and most of the world's energy demand is fulfilled from petroleum, coal and natural gas, which have shares of 31.1, 28.9 and 21.4 percent, respectively [4]. The demand of energy increases exponentially with the increase in population and change in lifestyle throughout the world [5]. Due to the speedy increases in population and industrialisation, tremendous exhaustion of fossil fuels has taken place. The 2017 International Energy Outlook reported that the estimated increase in consumption of fossil fuels from 2015 to 2040 will be 28% worldwide [6].

The ongoing increase in utilisation of non-renewable energy sources resulted in depletion of resources on the one hand, and also led to pollution of air, water and soil on

the other hand. To overcome this problem, research groups throughout the world are busy looking for sustainable, propagating and fuel-efficient energy sources [7]. Among the options, biomass is accepted as the most feasible and biologically friendly choice for sustainable power. It could diminish the dependence on the utilisation of non-renewable energy sources. Biomass's conversion to energy is a rapidly developing field of science and technology, and is expected to satisfy energy needs to a great extent [8].

There are various approaches to biomass's conversion into biofuel. Pyrolysis is one of them, which is a most productive thermo-chemical technique carried out in an inert atmosphere for the degradation of organic compounds [9]. These days pyrolysis is considered the ultimate choice, as it can produce various products, including solids, liquids and gases, depending on the operating parameters, e.g., temperature, catalyst and reaction time [10]. Catalyst and temperature are the two key parameters which play effective roles in product yield, and this has been reported in various studies. Shadangi and Mohanty [11] studied decomposition of karanja seeds at various temperatures using CaO, Al₂O₃ and kaolin as catalysts. Maximum bio-oil production was noticed at 550 °C, and kaolin performance was observed to be better than those of other catalysts.

Patra et al. [12] studied pyrolysis of *Delonix regia* seed and investigated the effects of temperature on composition and yield of bio-oil. At a temperature of 600 °C, a maximum oil yield of about 48% was reported. The bio-oil composition was studied with FTIR and GC-MS; and amides, nitriles, aldehydes and ketones were found to be the main components. Sun et al. [13] performed flash pyrolysis of rice husk and sawdust at 700–1000 °C in a flow reactor. The authors observed a rise in gas and reductions in char and liquid fractions as the temperature increased. Punsuwan et al. [14] examined the influences of temperature and particle size on the decomposition of palm kernels, palm shells and cassava pulp. They noticed that smaller particles and higher temperatures lowered the char yield and raised the gas yield. Natural materials in raw and modified forms, such as termite hill and anthill, have also been used as catalysts for enhanced bio-oil yield from the decomposition of waste biomass and production of biodiesel from edible and non-edible oils. Nisar et al. [15] used termite hill as the catalyst for enhanced bio-oil production from peanut shell waste, and conditions were optimized for maximum oil yield. In another study, Olubunmi et al. [16] successfully applied iron supported anthill for biodiesel yield from waste cooking oil. In yet another study, Yusuff [17] investigated the catalytic behaviour of alkaline modified anthill for biodiesel yield from *Chrysophyllum albidium* seed oil.

Apart from studying the oil yields from waste biomass, the kinetics of various biomass waste have also been studied in detail by various authors. In two separate studies, Torres-Garcia et al. [18] and Nisar et al. [15] studied in detail the kinetics of the pyrolysis of peanut shells. Using the Kissinger method, Torres-Garcia et al. reported the E_a values for non-catalytic reactions of hemicellulose, cellulose and lignin as 172.0, 203.4 and 218.0 kJ·mol⁻¹ respectively; and Nisar et al. reported the E_a values for catalytic reactions of hemicellulose, cellulose and lignin as 66.5, 74.8 and 133 kJ·mol⁻¹ respectively. In another study, Nisar et al. [19] studied the kinetics of the pyrolysis of sugarcane bagasse and evaluated the E_a values via Kissinger method for hemicellulose, cellulose and lignin, which were 99.8, 133.0 and 232.8 kJ·mol⁻¹, respectively, in the absence of catalyst; and 83.1, 99.8 and 116.4 kJ·mol⁻¹, respectively, in the presence of catalyst.

Enormous quantities of biomass waste from trees, bushes and crop harvest are produced throughout the globe. Numerous studies have been conducted on the transformation of biomass into bio-oil, but still, pyrolysis in combination with kinetics of karanja seed residue has not been yet studied [20]. Karanja tree (botanical name: *Pongamia pinnata* L. from the family Fabaceae; local name: Sukh Chain) is of average size with a height between 15 and 20 m and is evergreen. It grows in temperate and tropical regions of Asia, including some part of Pakistan, i.e., Sind and Punjab provinces [21]. Oil is extracted from the seeds and used for various purposes, and the de-oiled cake or seed residue is thrown away as waste. Thus, the use of this karanja seeds residue for bio-oil production through pyrolysis is a fascinating way to diminish the waste and produce some value-added products from it.

2. Experimental

2.1. Materials and Methods

In this study, the *Pongamia pinnata* L. press cake biomass was collected from an oil extraction facility in the local market of Faisalabad city, Punjab, Pakistan. The remaining oil in the press cake was extracted with pure n-hexane using a Soxhlet assembly. The de-oiled press cake thus obtained was dried and then grinded using a blender. The crushed biomass was then sieved through mesh number 35 to get suitably sized particles for pyrolysis studies. Abandoned anthill was collected from the soil around the trunk of an aged sheesham tree (*Dalbergia sissoo*) in village Hathian, District Mardan, Khyber Pakhtunkhwa, Pakistan. It was then ground into powder using a mortar and pestle and secured in a glass bottle at room temperature for future study. Acetone was regularly used to clean the condenser after each pyrolysis experiment.

2.2. Catalyst Characterisation

The structural features of anthill were determined through scanning electron microscopy. The micrographs were recorded using JEOL, JSM-5600 proprietary software on a Windows 95 platform to analyse the chemical composition of materials through EDX (JSM-IT-100 Japan). The surface area and porosity of anthill catalyst were investigated using a surface area and pore size analyser (NOVA2200e Quantachrome, Boynton Beach, FL, USA). The samples were examined to determine crystallinity using a JEOL, Japanese-made XRD, model JDX-3532. The crystalline phases in the test sample were identified using X'pert high score software. The compound composition of the catalyst was studied using a Shimadzu, Japanese-made XRF, model EDX-7000.

2.3. Pyrolysis Experiments

Pyrolysis of karanja press cake in the presence and absence of catalyst was carried out in a salt bath in an inert atmosphere. A schematic sketch of assembly has already been given in our previous communication [22]. A known weight of the karanja press cake was placed in a 100 mL Pyrex glass, immersed in molten salt, and linked to the condenser with the facility for collection of bio-oil. The oil obtained was characterized through GC-MS.

2.4. Kinetic Study

Thermogravimetry of the karanja press cake with and without anthill at temperature programme rates of 3, 7, 12, 20, and 30 °C·min⁻¹ was performed using a thermogravimetric analyser, Q500, equipped with DSC 8000. The data acquired were utilized for determining kinetic parameters by applying the Kissinger method. In this method, the reactant is heated at different temperature programme rates, and peak temperature is recorded at each heating rate. Plots are constructed of $\ln\beta/T_m^2$ vs. $1000/T_m$ using Equation (1).

$$\ln\left[\frac{\beta}{T_m^2}\right] = \ln\left(\frac{A \cdot R}{E_a}\right) - \frac{E_a}{RT_m} \quad (1)$$

where T_m is the highest decomposition temperature, β is the temperature programme rate, and R is the gas constant. E_a and A , which represent activation energy and frequency factor, were estimated from slopes and intercepts of the plots.

3. Results and Discussion

3.1. Characterisation of Catalyst

The XRF analysis of anthill was conducted, and the results revealed that anthill contains silica (SiO_2), alumina (Al_2O_3), iron oxide (Fe_2O_3), potassium oxide (K_2O), calcium oxide (CaO) and titanium oxide (TiO_2). Percentage compositions were 64.787%, 20.399%, 8.306%, 3.510%, 1.615%, and 1.039%, respectively. Some other compounds were also found in trace amounts. The results from XRF analysis are given in Table 1. The data are consonant with some reported work. Yusuff [17] examined the XRF analysis of anthill and found that

anthill is composed of silica (SiO_2), alumina (Al_2O_3), iron oxide (Fe_2O_3), potassium oxide (K_2O), and zirconia (ZrO_2).

Table 1. XRF of anthill displaying percentage compositions of various compounds in the sample.

S. No.	Compound	% Composition
01	SiO_2	64.787
02	Al_2O_3	20.399
03	Fe_2O_3	8.306
04	K_2O	3.510
05	CaO	1.615
06	TiO_2	1.039
07	MnO	0.166
07	V_2O_5	0.041
08	ZrO_2	0.039
09	Cr_2O_3	0.025
10	CuO	0.021
11	SrO	0.019
12	ZnO	0.016

XRD of anthill was performed, and the pattern is shown in Figure 1, which exhibits the presence of siliceous clay in abundance. The sharp peak at 26.66° predominantly represents quartz, whereas the other sharp peak at 20.89° was due to alumina. Another sharp peak at 50.23° was attributed to calcium alumino silicate [17]. Other small peaks in the diffractogram represent tridymite, cristobalite, kaolinite, etc. [23]. Moreover, X'pert High Score software was run on XRD data, and various metal oxides were identified with different crystalline phases: Oxides of silicon were quartz with a chemical formula of Si_3O_6 and a hexagonal crystal system [24]; mutinaite with a orthorhombic crystal system having chemical formula Si_9O_{19} ; magadiite with the formula $\text{Si}_{24}\text{O}_{52}$ and a hexagonal system [25]. Oxides of aluminium were nordstrandite, having a chemical formula of Al_2O_6 and anorthic crystal system [26]; and gibbsite, having a chemical formula of Al_3O_9 and a monoclinic crystal system [27]. Moreover, oxides of iron had various phases—i.e., goethite (Fe_4O_8) having an orthorhombic structure; schwertmannite ($\text{Fe}_{16}\text{O}_{32}$), having an anorthic crystal phase [28]; and maghemite ($\text{Fe}_{21}\text{O}_{32}$), having a cubic crystal system. Oxides of titanium were Ti_8O_{16} having an anorthic crystal system [29], and $\text{Ti}_{12}\text{O}_{20}$, having a monoclinic crystalline structure [30].

The surface morphology of anthill was investigated using SEM, as illustrated in Figure 2. The structure of anthill shown in Figure 2 clearly has an irregular and rough texture with agglomerated particles. The fractures and pores are frequently visible on the anthill surface, and these provide a mesoporous structure to the material, facilitating the occurrence of the degrading reaction. The outcomes are in accordance with several previous studies. Yusuff et al. [31] used TiO_2 /anthill as a heterogeneous catalyst for photocatalytic degradation of textile waste water. They observed rough, irregular, and agglomerated particles in the SEM image of raw anthill. In another study, Yusuff et al. [23] used zinc-modified anthill for biodiesel production from used cooking oil, and reported that the raw anthill had a rough surface with small and large particles in the SEM image.

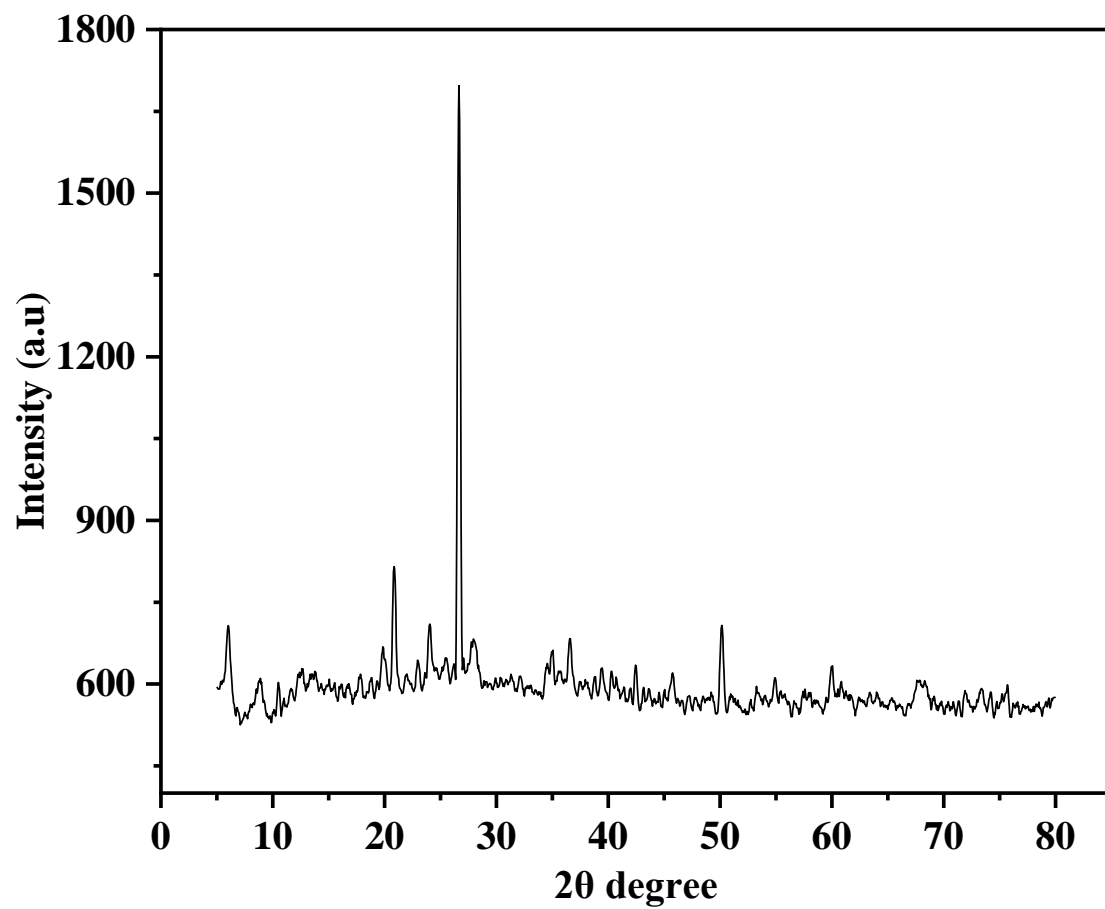


Figure 1. XRD patterns of anthill.

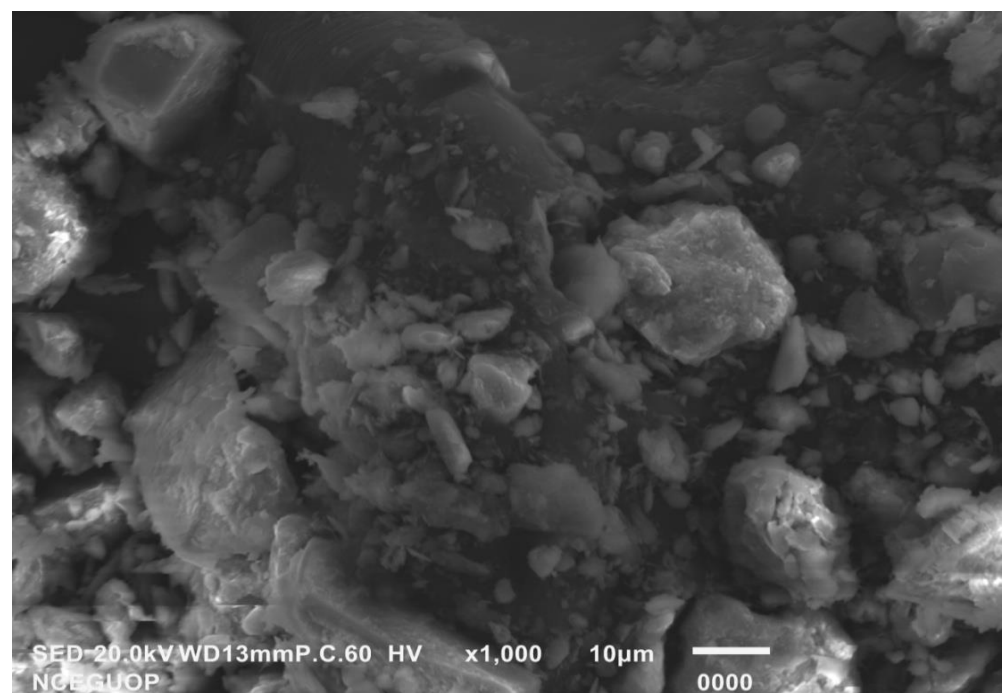


Figure 2. SEM image of anthill catalyst.

The EDX of the anthill catalyst shown in Figure 3 reveals that anthill consists mostly of silicon (Si), aluminium (Al), and oxygen (O), along with iron (Fe), calcium (Ca), potassium (K), magnesium (Mg), etc. The data agree well with some studies. Yusuff et al. [31] applied TiO_2 /anthill for photodegradation of textile wastewater. The EDX analysis of anthill exhibited that it consists of silicon (49.20%), aluminium (20.14%), oxygen (12.49%), and calcium (12.17%).

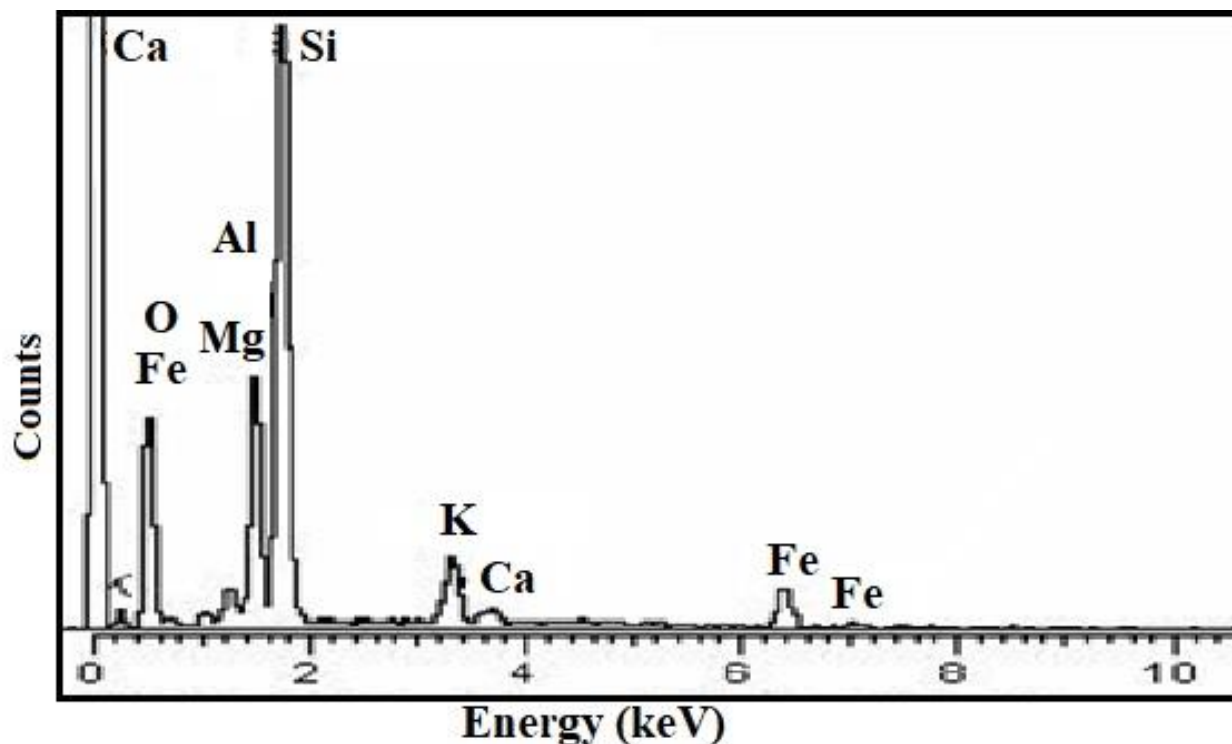


Figure 3. EDX of anthill catalyst.

The catalyst was subjected to a surface area and pore size analysis to identify the surface nature of the catalyst, including pore volume, surface area, and pore radius. The surface area and pore volume of anthill were $25.065 \text{ m}^2/\text{g}$ and 0.014 cc/g , respectively, using the Barrett–Joyner–Halenda adsorption technique, whereas pore radius of anthill was observed to be 17.015 \AA . The comprehensive surface activities of the catalyst were determined using the Brunauer–Emmet–Teller surface area analysis method, and the surface area of anthill was found to be $34.637 \text{ m}^2/\text{g}$. These findings are in consonance with some previous studies. Yusuff and Adesina [32] investigated the characterisation and adsorption properties of anthill for dye removal from aqueous solutions. The textural analysis of the anthill was studied through Brunauer–Emmet–Teller (BET), t-plot, and Dubinin–Radushkevich (DR) techniques; and total pore volume, pore diameter, and surface area of the activated anthill were observed to be $0.0227 \text{ cm}^3/\text{g}$, 12.46 \AA and $48.12 \text{ m}^2/\text{g}$ respectively.

3.2. Pyrolysis and Characterisation of Products

In order to study temperature's impact on the pyrolysis of waste karanja seed press cake, the pyrolysis experiment in the absence and presence of 5% anthill as the catalyst were carried out for 30 min at intervals of $10 \text{ }^\circ\text{C}$ from $310 \text{ }^\circ\text{C}$ to $400 \text{ }^\circ\text{C}$. The obtained pyrolysates without and with catalyst, i.e., bio-oil, char, and gas, are shown in Figure 4a,b respectively. Figure 4a shows that the amount of oil obtained as a result of the non-catalytic pyrolysis steadily increased until it reached a maximum at $360 \text{ }^\circ\text{C}$. Furthermore, the amount of oil tended to decrease with the increase in temperature; therefore, $360 \text{ }^\circ\text{C}$ was noted as the optimal temperature for peak yield of bio-oil without catalyst. The figure also shows that when the temperature rises, the gaseous percentage increases and the bio-char fraction

decreases, which is ascribed to secondary breakdown of bio-oil [33]. Figure 4b presents the catalytic degradation at various temperatures. As is evident from the plot, the production of liquid product progressively rose up to 340 °C, and finally declined above 340 °C. As a result, 340 °C is the ideal temperature for oil production. The production of gaseous products progressively increased with the increase in temperature. This demonstrates how anthill as a catalyst has lowered the optimal temperature for bio-oil yield from karanja press cake.

The oil collected at optimized conditions in the absence of catalyst was analysed with GC-MS. The detected compounds are displayed in Table 2. The compounds detected in the bio-oil included aromatic, aliphatic, closed chain, branched chain, saturated, and unsaturated hydrocarbons ranging from C₅ to C₁₉. The major compounds identified were furan, 2-methoxy, 2-furanmethanol, isosorbide, 4-piperidinamine, N,1-dimethyl, 3-octanamine and phenols, followed by other hydrocarbons in trace quantities. Almost the same results were reported by other researchers [34–36]. Soongpravit et al. [35] studied bio-oil obtained from the decomposition of *Millettia (Pongamia pinnata)* seed waste through GC-MS, and the bio-oil was found to be composed mainly of ester, ketones, carboxylic acid, and N- compounds. Aliphatic hydrocarbons were also noticed. Dhanavath et al. [36] reported that the bio-oil obtained from pyrolysis of karanja seed press cake through liquification contained phenols, carboxylic acid, and carbonyls. Moreover, unsaturated and saturated fatty acid and methyl ester fatty acid were also reported.

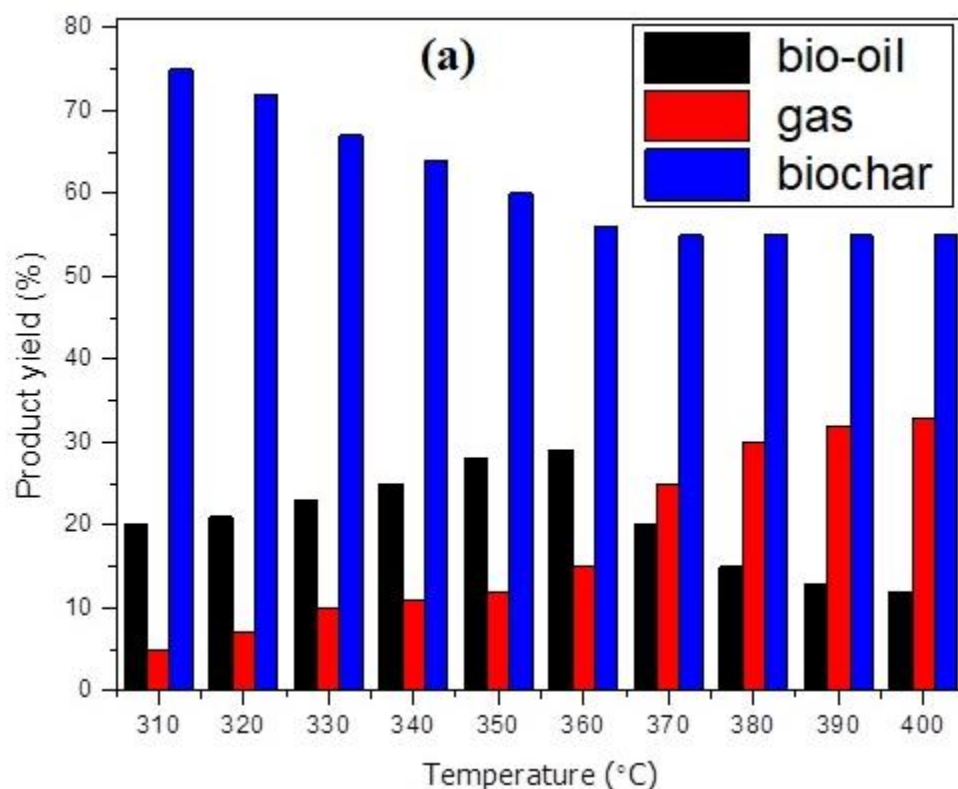


Figure 4. Cont.

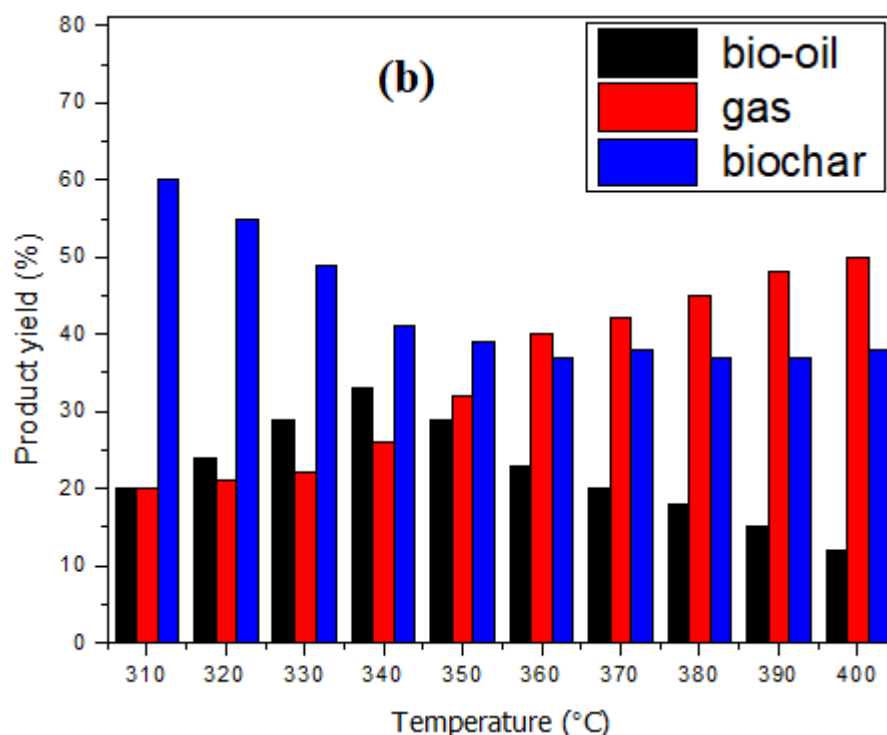


Figure 4. Optimisation of temperature (a) without catalyst (b) with catalyst.

The pyrolyzed products recovered from decomposition of karanja seed residue at optimal conditions in the presence of 5% anthill were collected and examined through GC-MS. Table 3 provides comprehensive details of all the products, including their formulas, names, molecular weights, percent areas, and retention times. There were about 42 hydrocarbons (that were detected) which had C_2 – C_{63} carbon chains. Comparing catalytic pyrolyzed products of karanja seed press cake with the non-catalytic products shown in Tables 2 and 3 reveals that the catalyst has a great impact not only by increasing the number of compounds, but also enhancing the quantity of oil obtained [37,38]. The major compounds identified were 2-furanmethanol, 2-n-butyl furan, didemnin B, 1,2-cyclopentanedione-3-methyl, phenols, 1,3-isobutylhexahydropyrrolo[1,2-a]pyrazine-1,4-dione, 5,10-diethoxy-2,3,7,8-tetrahydro-H,6H-dipyrrolo[1,2,1,2]pyrazine, pyrrole[1,2-a]pyrazine-1,4-dione, hexahydro-3-(2-methylpropyl)-oleic acid, butanamide, and 3-methyl,2(5H)-furan-4-one. Almost the same results were reported by other researchers. Shadangi and Mohanty [11] studied the decomposition of karanja seed over CaO and Al_2O_3 to produce bio-oil. They found that the catalyst played an important role by increasing the quantity and quality of the compounds obtained. The major components obtained were furan, alkanes, phenol, acids, esters, hexane, laevoglucose, amide, nitriles, and benzene. The results in this study show that the catalyst removed the undesired compounds, and also increased the yield of hydrocarbons in the bio-oil. These observations are in accordance with the argument put forwarded by Bhoi et al. [39]. Moreover, the GC-MS of the bio-oil produced from catalytic decomposition of de-oiled karanja press cake shows that it is rich with components such as alcohols, phenols, furfural, maltol, oleic acid, and esters, which indicates that the quality of bio-oil improved, making it a potential candidate for biofuel. These findings are in consonance with the results of Zhang et al. [37]. The authors noted high yields of aromatic compounds and phenols as a result of catalytic pyrolysis of bio-waste.

Table 2. Compounds detected in bio-oil obtained from karanja seed press cake without catalyst.

S. No.	R/T	Component	Chem. Formula	Mol. wt.	Area%
1	2.40	Furan, 2-methoxy	C ₅ H ₆ O ₂	98	46.79
2	3.20	2-Furanmethanol	C ₅ H ₆ O ₂	98	12.78
3	3.67	3-Octanamine	C ₈ H ₁₉ N	129	3.28
4	4.67	E-2-Tetradecen-1-ol	C ₁₄ H ₂₈ O	212	0.19
5	5.34	Phenol	C ₆ H ₆ O	94	2.67
6	5.93	Sorbic Acid	C ₆ H ₈ O ₂	112	0.94
7	6.42	1,2,3-Trimethylpiperidin-4-one	C ₈ H ₁₅ NO	141	1.69
8	6.78	Phenol, 4-methyl	C ₇ H ₈ O	108	1.22
9	7.01	2,5-Heptadien-4-one,2,6-dimethyl	C ₉ H ₁₄ O	138	1.55
10	7.68	Glycyl-D-asparagine	C ₆ H ₁₁ N ₃ O ₄	189	1.97
11	8.48	3,4-Dihydro-1-methylpyrrolo[1,2a]pyrazine	C ₈ H ₁₀ N ₂	134	2.81
12	9.15	4-Piperidinamine, N,1-dimethyl	C ₇ H ₁₆ N ₂	128	6.77
13	9.60	Tricyclo[4.3.1.1(3,8)]undecan-1amine	C ₁₁ H ₁₉ N	165	0.09
14	10.27	Indole	C ₈ H ₇ N	117	1.45
15	11.16	Isosorbide	C ₆ H ₁₀ O ₄	146	8.67
16	11.69	1H-Indole, 3-methyl	C ₉ H ₁₇ N	131	0.70
17	12.06	1,3;2,4-Di-O-methylene-d-arabitol	C ₇ H ₁₂ O ₅	176	0.61
18	12.41	Acetic acid,2-(1,2,3,4-tetrahydro6methyl-2,4dioxo-5pyrimidylmethylthio	C ₈ H ₁₀ N ₂ O ₄ S	230	0.52
19	13.30	à-[2[NAziridyl]ethylamino]isobutyronitrile	C ₈ H ₁₅ N ₃	153	0.89
20	14.83	2H-1-Benzopyran, 7-methoxy-2,2-dimethyl	C ₁₂ H ₁₄ O ₂	190	0.19
21	16.56	9,10a-dimethyl-6-methylene-3á-isopropyl	C ₂₀ H ₃₂ O ₂	304	0.05
22	17.05	Benzeneethanamine, 3-hydroxy-4-methoxy	C ₉ H ₁₃ NO ₂	167	0.38
23	17.62	á-Himachalenoxide	C ₁₅ H ₂₄ O	220	0.19
24	17.85	Dimethoxyamphetamine, 2,5-	C ₁₁ H ₁₇ NO ₂	195	0.14
25	18.33	N-(O-Nitrophenylthio)-l-leucine	C ₁₂ H ₁₆ N ₂ O ₄ S	284	0.14
26	18.66	Pyrrolo[1,2]pyrazine-1,4-dione, hexahydro-3-(2-methylpropyl)-	C ₁₁ H ₁₈ N ₂ O ₂	210	0.09
27	19.35	5,10-Diethoxy-2,3,7,8-tetrahydro-H,6H-dipyrrolo[1,2,1,2]pyrazine	C ₁₄ H ₂₂ N ₂ O ₂	250	1.22
28	20.35	8-Octadecenoic acid, methyl ester	C ₁₉ H ₃₆ O ₂	296	0.89
29	23.49	2-[5-(2-Methyl-benzooxazol-7-yl)1H-pyrazol-3-yl]-phenol	C ₁₇ H ₁₃ N ₃ O ₂	291	0.89

Table 3. Composition of oil obtained from karanja seed press cake with catalyst.

S. No.	R/T	Component	Chem. Formula	Mol. wt	Area %
1	7.12	Piperidine, 1-methyl-	C ₆ H ₁₃ N	99	2.51
2	7.52	Acetamide	C ₂ H ₅ NO	59	4.73
4	7.84	2,3-Butanediol	C ₄ H ₁₀ O ₂	90	1.98
5	10.39	2-Furanmethanol	C ₅ H ₆ O ₂	98	32.15
6	10.92	Acetamide, N,N-dimethyl-	C ₄ H ₉ NO	87	1.39
7	12.05	2-n-Butyl furan	C ₈ H ₁₂ O	124	16.84
8	12.62	2(5H)-Furanone	C ₄ H ₄ O ₂	84	5.01
9	13.05	[1,3,4]Thiadiazol, 2-amino-5-(2-piperidin-1-ylethyl)-	C ₉ H ₁₆ N ₄ S	244	0.71
10	13.83	3(2H)-Furanone, 2-(1-hydroxy-1-methyl-2-oxopropyl)-2,5-dimethyl-	C ₁₀ H ₁₄ O ₄	198	0.96
11	14.15	Mannosamine	C ₆ H ₁₃ NO ₅	179	0.66
12	15.26	Phenol	C ₆ H ₆ O	94	9.27
13	16.1	Butanamide, 3-methyl-	C ₅ H ₁₁ NO	101	5.22
14	16.93	1,2-Cyclopentanedione, 3-methyl-	C ₆ H ₈ O ₂	112	9.77
15	17.21	Formamide, N-[1-[(1-cyano-2-methylpropyl)hydroxyamino]ethyl]-	C ₈ H ₁₅ N ₃ O ₂	185	2.57

Table 3. Cont.

S. No.	R/T	Component	Chem. Formula	Mol. wt	Area %
16	18.07	Ethanone, 1-(1H-pyrrol-2-yl)-	C ₆ H ₇ NO	109	2.81
17	19.24	2-Vinyl-9-[3-deoxy-β-d-ribofuranosyl]hypoxanthine	C ₁₂ H ₁₄ N ₄ O ₄	278	4.96
18	19.87	Maltol	C ₆ H ₆ O ₃	126	12
19	23.39	1,2-Benzenediol	C ₆ H ₆ O ₂	110	3.38
20	25.04	Acetic acid, 2-[2-methyl-4-(1-piperidylmethyl)-1,3-dioxolan-2-yl]-, ethyl ester	C ₁₄ H ₂₅ NO ₄	271	5.12
21	25.81	Isosorbide	C ₆ H ₁₀ O ₄	146	1.00
22	28.11	Dodecanoic acid, 3-hydroxy-	C ₁₂ H ₂₄ O ₃	216	8.11
23	33.36	Cholestan-3-ol, 2-methylene-, (3β,5α)-	C ₂₈ H ₄₈ O	400	3.99
24	34.14	2-Methylenecholestan-3-	C ₂₈ H ₄₈ O	400	2.94
25	36.31	Uric acid	C ₅ H ₄ N ₄ O ₃	168	0.39
26	37.04	Nitro-L-arginine	C ₆ H ₁₃ N ₅ O ₄	219	6.8
27	37.44	Propyl-3,6-diazahomoadamantan-9-ol	C ₁₂ H ₂₂ N ₂ O	210	1.3
28	40.32	Didemnin B	C ₅₇ H ₈₉ N ₇ O ₁₅	1112	15.14
29	42.85	Actinomycin C2	C ₆₃ H ₈₈ N ₁₂ O ₁₆	1268	5.57
30	43.71	1,3-Isobutylhexahydropyrrolo[1,2-a]pyrazine-1,4-dione	C ₁₁ H ₁₈ N ₂ O ₂	210	9.17
31	44.01	5,10-Diethoxy-2,3,7,8-tetrahydro-1H,6H-dipyrrolo[1,2-a;1',2'-d]pyrazine	C ₁₄ H ₂₂ N ₂ O ₂	250	7.9
32	44.4	Pyrrolo[1,2-a]pyrazine-1,4-dione, hexahydro-3-(2-methylpropyl)-	C ₁₁ H ₁₈ N ₂ O ₂	210	7.58
33	56.24	Oleic Acid	C ₁₈ H ₃₄ O ₂	282	7.09
34	61.72	Ethyl iso-allocholate	C ₂₆ H ₄₄ O ₅	436	0.61
35	61.87	Ergotaman-3,6,18-trione,9,10-dihydro-12-hydroxy-2-methyl-5'-(phenylmethyl)-(5'α,10α)	C ₃₃ H ₃₇ N ₅ O ₅	583	2.71
36	62.07	Didemnin B	C ₅₇ H ₈₉ N ₇ O ₁₅	1112	0.33
37	62.16	Oxiraneoctanoic acid, 3-octyl cis-	C ₁₈ H ₃₄ O ₃	298	0.7
38	62.58	Pregn-4-ene-3,20-dione,17,21-dihydroxy,bis(O-methylxime)	C ₂₃ H ₃₆ N ₂ O ₄	404	1.77
39	63.11	Phenol, 2,2'-methylenebis[6-(1,1-dimethylethyl)-4-methyl-	C ₂₃ H ₃₂ O ₂	340	2.57
40	64.63	1,2-Benzenedicarboxylic acid, diisooctyl ester	C ₂₄ H ₃₈ O ₄	390	3.94
41	65.54	9,10-Anthracenedione, 1,2,3,4-tetrahydro-1,2,3,4,5-pentahydroxy-7-methoxy-2-methyl-, (1α,2β,3β,4α)-	C ₁₆ H ₁₆ O ₈	336	3.08
42	65.77	2-[5-(2-Methyl-benzooxazol-7-yl)-1H-pyrazol-3-yl]-phenol	C ₁₇ H ₁₃ N ₃ O ₂	291	5.21

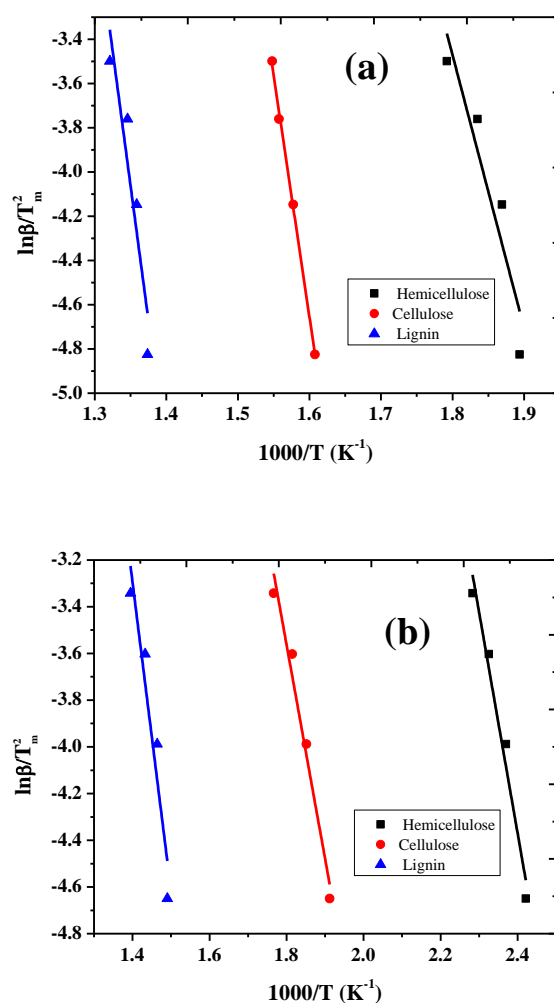
3.3. Kinetic Study of Karanja Seed Press Cake Pyrolysis

Thermogravimetric analysis of thermal degradation of karanja seed press cake in the presence and absence of anthill at temperature programme rates of 3, 12, 20, and 30 °C·min⁻¹ was performed, and the acquired data were used for determining kinetic parameters of the pyrolysis reaction using the Kissinger equation. Plots of lnB/T_m² vs. 1000/T_m were constructed by applying the Kissinger equation to the data obtained from the thermal degradation of karanja seed press cake with/without anthill, and the results are shown in Figure 5a,b. The activation energy and frequency factor for catalytic and non-catalytic samples were determined from the slopes and intercepts of plots, and these are listed in Table 4. The Ea values in the absence of catalyst for hemicellulose, cellulose, and lignin decomposition were determined as 99.7 ± 0.4, 182.9 ± 0.5, and 199.5 ± 0.7 kJ·mol⁻¹; with catalyst they were 74.8 ± 0.2, 83.1 ± 0.4, and 108.0 ± 0.5 kJ·mol⁻¹, respectively. As Ea values for non-catalytic degradation were found to be higher than catalytic ones, the catalytic efficiency of anthill is enough for it to be considered a suitable catalyst for the decomposition of biomass waste. The results agree well with some reported studies.

Table 4. Kinetic parameters calculated by applying the Kissinger method.

Component	Catalytic Reaction			Non-Catalytic Reaction		
	Ea (kJ·mol ⁻¹)	A (min ⁻¹)	R ²	Ea (kJ·mol ⁻¹)	A (min ⁻¹)	R ²
Hemicellulose	99.7 ± 0.4	4.8 × 10 ⁸	0.859	74.8 ± 0.2	6.5 × 10 ⁶	0.958
Cellulose	182.9 ± 0.5	8.4 × 10 ¹³	0.996	83.1 ± 0.4	2.3 × 10 ⁸	0.962
Lignin	199.5 ± 0.7	9.7 × 10 ¹⁴	0.848	108.0 ± 0.5	8.8 × 10 ⁹	0.872

Nisar et al. [15] performed peanut shell decomposition with/without termite hill and investigated the kinetic parameters by using thermogravimetric data. Using the Kissinger method, they found Ea values in the absence of catalyst for hemicellulose, cellulose, and lignin degradation of 108.1, 116.4, and 182.9 kJ·mol⁻¹, respectively; and in case of catalytic pyrolysis, the Ea values were computed to be 66.5, 74.8, and 133 kJ·mol⁻¹, respectively. In another study, Nisar et al. [19] carried out the kinetic study of sugarcane bagasse and evaluated the kinetic parameters of catalysed and non-catalysed reactions. Using the Kissinger method, they observed lower Ea values for catalysed decomposition of hemicellulose, cellulose, and lignin, i.e., 83.1, 99.8, and 116.4 kJ·mol⁻¹ as compared to un-catalysed reactions, i.e., 99.8, 133, and 232.8 kJ·mol⁻¹. Torres-Garcia et al. [18] carried out pyrolysis of peanut shells, and by applying the Kissinger method, they observed activation energies for hemicellulose, cellulose, and lignin degradation of 172, 203.4, and 218 kJ·mol⁻¹, respectively.

**Figure 5.** Plots constructed from decomposition of karanja press cake applying the Kissinger method: (a) in absence of catalyst; (b) in presence of catalyst.

4. Conclusions

In this study, karanja seed press cake was pyrolyzed with/without anthill as a catalyst. TG analysis of karanja seed press cake was carried out with and without catalyst in the inert atmosphere at temperature programme rates of 3, 12, 20, and 30 °C·min⁻¹. Kinetic parameters were determined from the TG data by applying the Kissinger equation. The Kissinger equation gave activation energy values for hemicellulose, cellulose, and lignin of 99.7 ± 0.4, 182.9 ± 0.5, and 199.5 ± 0.7 kJ·mol⁻¹ without catalyst; and with catalyst, they were 74.8 ± 0.2, 83.1 ± 0.4, and 108.0 ± 0.5 kJ·mol⁻¹. Moreover, pyrolysis experiments were carried out without and with anthill catalyst in an indigenously made furnace in nitrogen, at 310–400 °C. The pyrolyzed oil collected at the optimized temperature was analysed through GC-MS. From the results, it has been concluded that anthill as a catalyst not only enhanced the quality and quantity of the pyrolyzed oil, but also reduced the temperatures of maximum degradation and activation energy. From the results, it was also deduced that the oil obtained from the de-oiled karanja seed press cake can be used as fuel if upgraded properly.

Author Contributions: J.N.: conceptualisation, funding acquisition, resources, project administration. S.W.: investigation, methodology, writing—original draft. A.S.: visualisation, writing—review and editing. F.A.: sample collection and treatment. G.A. and F.M.: writing, results, analysis. A.A.: writing—review and editing. All authors have read and agreed to the published version of the manuscript.

Funding: J.N. acknowledges the support of the Higher Education Commission of Pakistan through grant number 20–1491.

Institutional Review Board Statement: Not applicable.

Informed Consent Statement: Not applicable.

Data Availability Statement: Not applicable.

Conflicts of Interest: Authors have no conflicts of interest.

References

1. Demirbas, A. Recent advances in biomass conversion technologies. *Energy Educ. Sci. Technol.* **2000**, *6*, 19–40.
2. Zinkle, S.J.; Was, G.S. Materials challenges in nuclear energy. *Acta Mater.* **2013**, *61*, 735–758. [[CrossRef](#)]
3. Iqbal, J.; Howari, F.; Mohamed, A.-M.; Paleologos, E. Assessment of Radiation Pollution from Nuclear Power Plants. In *Pollution Assessment for Sustainable Practices in Applied Sciences and Engineering*; Elsevier: Amsterdam, The Netherlands, 2021; pp. 1027–1053.
4. Alhumade, H.; da Silva, J.C.G.; Ahmad, M.S.; Çakman, G.; Yıldız, A.; Ceylan, S.; Elkamel, A. Investigation of pyrolysis kinetics and thermal behavior of Invasive Reed Canary (*Phalaris arundinacea*) for bioenergy potential. *J. Anal. Appl. Pyrolysis* **2019**, *140*, 385–392. [[CrossRef](#)]
5. Mishra, R.K.; Mohanty, K. Pyrolysis characteristics, fuel properties, and compositional study of Madhuca longifolia seeds over metal oxide catalysts. *Biomass Convers. Biorefinery* **2019**, *10*, 1–17. [[CrossRef](#)]
6. Das, B.; Mohanty, K. A review on advances in sustainable energy production through various catalytic processes by using catalysts derived from waste red mud. *Renew. Energy* **2019**, *143*, 1791–1811. [[CrossRef](#)]
7. Gupta, S.; Gupta, G.K.; Mondal, M.K. Slow pyrolysis of chemically treated walnut shell for valuable products: Effect of process parameters and in-depth product analysis. *Energy* **2019**, *181*, 665–676. [[CrossRef](#)]
8. Nisar, J.; Ali, G.; Ullah, N.; Awan, I.A.; Iqbal, M.; Shah, A.; Sirajuddin; Sayed, M.; Mahmood, T.; Khan, M.S. Pyrolysis of waste tire rubber: Influence of temperature on pyrolysates yield. *J. Environ. Chem. Eng.* **2018**, *6*, 3469–3473. [[CrossRef](#)]
9. Czajczyńska, D.; Anguilano, L.; Ghazal, H.; Krzyżyńska, R.; Reynolds, A.; Spencer, N.; Jouhara, H. Potential of pyrolysis processes in the waste management sector. *Therm. Sci. Eng. Prog.* **2017**, *3*, 171–197. [[CrossRef](#)]
10. Chowdhury, R.; Sarkar, A. Reaction Kinetics and Product Distribution of Slow Pyrolysis of Indian Textile Wastes. *Int. J. Chem. React. Eng.* **2012**, *10*, 456. [[CrossRef](#)]
11. Shadangi, K.P.; Mohanty, K. Thermal and catalytic pyrolysis of Karanja seed to produce liquid fuel. *Fuel* **2014**, *115*, 434–442. [[CrossRef](#)]
12. Patra, S.C.; Vijay, M.; Panda, A.K. Production and characterisation of bio-oil from Gold Mohar (*Delonix regia*) seed through pyrolysis process. *Int. J. Ambient Energy* **2016**, *38*, 788–793. [[CrossRef](#)]
13. Sun, S.; Tian, H.; Zhao, Y.; Sun, R.; Zhou, H. Experimental and numerical study of biomass flash pyrolysis in an entrained flow reactor. *Bioresour. Technol.* **2010**, *101*, 3678–3684. [[CrossRef](#)] [[PubMed](#)]

14. Punsuwan, N.; Tangsathitkulchai, C. Product Characterization and Kinetics of Biomass Pyrolysis in a Three-Zone Free-Fall Reactor. *Int. J. Chem. Eng.* **2014**, *2014*, 1–10. [[CrossRef](#)]
15. Nisar, J.; Ahmad, A.; Ali, G.; Rehman, N.U.; Shah, A.; Shah, I. Enhanced Bio-Oil Yield from Thermal Decomposition of Peanut Shells Using Termite Hill as the Catalyst. *Energies* **2022**, *15*, 1891. [[CrossRef](#)]
16. Olubunmi, B.E.; Karmakar, B.; Aderemi, O.M.; Auta, M.; Halder, G. Parametric optimization by Taguchi L9 approach towards biodiesel production from restaurant waste oil using Fe-supported anthill catalyst. *J. Environ. Chem. Eng.* **2020**, *8*, 104288. [[CrossRef](#)]
17. Yusuff, A.S. Characterization of alkaline modified anthill and investigation of its catalytic behaviour in transesterification of Chrysophyllum albidum seed oil. *South Afr. J. Chem. Eng.* **2019**, *29*, 24–32. [[CrossRef](#)]
18. Torres-García, E.; Ramírez-Verduzco, L.; Aburto, J. Pyrolytic degradation of peanut shell: Activation energy dependence on the conversion. *Waste Manag.* **2020**, *106*, 203–212. [[CrossRef](#)]
19. Nisar, J.; Nasir, U.; Ali, G.; Shah, A.; Farooqi, Z.H.; Iqbal, M.; Shah, M.R. Kinetics of pyrolysis of sugarcane bagasse: Effect of catalyst on activation energy and yield of pyrolysis products. *Cellulose* **2021**, *28*, 7593–7607. [[CrossRef](#)]
20. Harreh, D.; Saleh, A.A.; Reddy, A.N.R.; Hamdan, S. An Experimental Investigation of Karanja Biodiesel Production in Sarawak, Malaysia. *J. Eng.* **2018**, *2018*, 1–8. [[CrossRef](#)]
21. Mukta, N.; Sreevalli, Y. Propagation techniques, evaluation and improvement of the biodiesel plant, *Pongamia pinnata* (L.) Pierre—A review. *Ind. Crop. Prod.* **2010**, *31*, 1–12. [[CrossRef](#)]
22. Nisar, J.; Rahman, A.; Ali, G.; Shah, A.; Farooqi, Z.H.; Bhatti, I.A.; Iqbal, M.; Rehman, N.U. Pyrolysis of almond shells waste: Effect of zinc oxide on kinetics and product distribution. *Biomass Convers. Biorefinery* **2020**, *12*, 2583–2595. [[CrossRef](#)]
23. Yusuff, A.S.; Gbadamosi, A.O.; Popoola, L.T. Biodiesel production from transesterified waste cooking oil by zinc-modified anthill catalyst: Parametric optimization and biodiesel properties improvement. *J. Environ. Chem. Eng.* **2021**, *9*, 104955. [[CrossRef](#)]
24. Taylor, J.; Miller, S.; Bibby, D. A Study of Decomposition Methods for Refinement of H⁺-ZSM5 Zeolite with Powder Diffraction Data. *Zeitschrift für Kristallographie-Crystalline Mater.* **1986**, *176*, 183–192. [[CrossRef](#)]
25. Garcés, J.M.; Rocke, S.C.; Crowder, C.E.; Hasha, D.L. Hypothetical Structures of Magadiite and Sodium Octosilicate and Structural Relationships Between the Layered Alkali Metal Silicates and the Mordenite-and Pentasil-Group Zeolites. *Clays Clay Miner.* **1988**, *36*, 409–418. [[CrossRef](#)]
26. Bosmans, H. Unit cell and crystal structure of nordstrandite, Al(OH)₃. *Acta Crystallogr. Sect. B Struct. Crystallogr. Cryst. Chem.* **1970**, *26*, 649–652. [[CrossRef](#)]
27. Wang, S.-L.; Johnston, C.T. Assignment of the structural OH stretching bands of gibbsite. *Am. Miner.* **2000**, *85*, 739–744. [[CrossRef](#)]
28. Fernandez-Martinez, A.; Timon, V.; Roman-Ross, G.; Cuello, G.; Daniels, J.; Ayora, C. The structure of schwertmannite, a nanocrystalline iron oxyhydroxysulfate. *Am. Miner.* **2010**, *95*, 1312–1322. [[CrossRef](#)]
29. Erdman, N.; Warschkow, O.; Asta, M.; Poeppelmeier, K.R.; Ellis, D.E.; Marks, L.D. Surface structures of SrTiO₃ (001): A TiO₂-rich reconstruction with ac (4 × 2) unit cell. *J. Am. Chem. Soc.* **2003**, *125*, 10050–10056. [[CrossRef](#)]
30. Andersson, S.; Collén, B.; Kruuse, G.; Kuylentierna, U.; Magnéli, A.; Pestmalis, H.; Asbrink, S. Identification of Titanium Oxides by X-Ray Powder Patterns. *Acta Chem. Scand.* **1957**, *11*, 1653–1657. [[CrossRef](#)]
31. Yusuff, A.S.; Olateju, I.I.; Adesina, O.A. TiO₂/anthill clay as a heterogeneous catalyst for solar photocatalytic degradation of textile wastewater: Catalyst characterization and optimization studies. *Materialia* **2019**, *8*, 100484. [[CrossRef](#)]
32. Yusuff, A.S.; Adesina, O.S. Characterization and adsorption behaviour of anthill for the removal of anionic dye from aqueous solution. *Int. J. Environ. Sci. Technol.* **2019**, *16*, 3419–3428. [[CrossRef](#)]
33. Westerhof, R.J.M.; Brilman, D.W.F.; Swaaij, W.P.M.; Kersten, S.R.A. Effect of Temperature in Fluidized Bed Fast Pyrolysis of Biomass: Oil Quality Assessment in Test Units. *Ind. Eng. Chem. Res.* **2009**, *49*, 1160–1168. [[CrossRef](#)]
34. Nayan, N.K.; Kumar, S.; Singh, R. Characterization of the liquid product obtained by pyrolysis of karanja seed. *Bioresour. Technol.* **2012**, *124*, 186–189. [[CrossRef](#)]
35. Soongpravit, K.; Sricharoenchaikul, V.; Atong, D. Pyrolysis of Millettia (*Pongamia*) *pinnata* waste for bio-oil production using a fly ash derived ZSM-5 catalyst. *J. Anal. Appl. Pyrolysis* **2019**, *139*, 239–249. [[CrossRef](#)]
36. Dhanavath, K.N.; Islam, M.S.; Bankupalli, S.; Bhargava, S.K.; Shah, K.; Parthasarathy, R. Experimental investigations on the effect of pyrolytic bio-oil during the liquefaction of Karanja Press Seed Cake. *J. Environ. Chem. Eng.* **2017**, *5*, 4986–4993. [[CrossRef](#)]
37. Zhang, B.; Zhong, Z.; Min, M.; Ding, K.; Xie, Q.; Ruan, R. Catalytic fast co-pyrolysis of biomass and food waste to produce aromatics: Analytical Py-GC/MS study. *Bioresour. Technol.* **2015**, *189*, 30–35. [[CrossRef](#)] [[PubMed](#)]
38. Xin, X.; Pang, S.; Mercader, F.D.M.; Torr, K.M. The effect of biomass pretreatment on catalytic pyrolysis products of pine wood by Py-GC/MS and principal component analysis. *J. Anal. Appl. Pyrolysis* **2018**, *138*, 145–153. [[CrossRef](#)]
39. Bhoi, P.; Ouedraogo, A.; Soloiu, V.; Quirino, R. Recent advances on catalysts for improving hydrocarbon compounds in bio-oil of biomass catalytic pyrolysis. *Renew. Sustain. Energy Rev.* **2020**, *121*, 109676. [[CrossRef](#)]